

## Phosphatase-Mediated Hydrolysis of Linear Polyphosphates

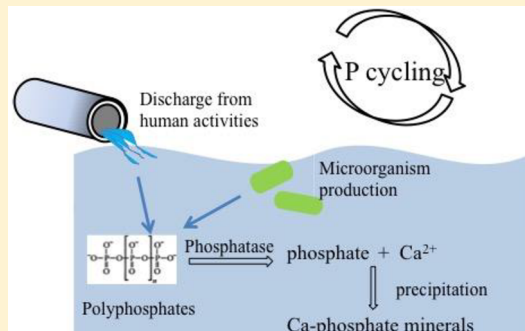
Rixiang Huang,<sup>†,#</sup> Biao Wan,<sup>†,#</sup> Margot Hultz,<sup>†</sup> Julia M. Diaz,<sup>‡</sup> and Yuanzhi Tang<sup>\*,†,‡</sup>

<sup>†</sup>School of Earth and Atmospheric Sciences, Georgia Institute of Technology, Atlanta, Georgia 30324-0340, United States

<sup>‡</sup>Department of Marine Sciences, Skidaway Institute of Oceanography, University of Georgia, Savannah, Georgia 31411, United States

### Supporting Information

**ABSTRACT:** Polyphosphates are a group of phosphorus (P) containing molecules that are produced by a wide range of microorganisms and human activities. Although polyphosphates are ubiquitous in aquatic environments and are of environmental significance, little is known about their transformation and cycling. This study characterized the polyphosphate-hydrolysis mechanisms of several representative phosphatase enzymes and evaluated the effects of polyphosphate chain length, light condition, and calcium ( $\text{Ca}^{2+}$ ).  $^{31}\text{P}$  nuclear magnetic resonance (NMR) spectroscopy was used to monitor the dynamic changes of P molecular configuration during polyphosphate hydrolysis and suggested a terminal-only degradation pathway by the enzymes. Such mechanism enabled the quantification of the hydrolysis rates by measuring orthophosphate production over time. At the same initial concentration of polyphosphate molecules, the hydrolysis rates were independent of chain length. The hydrolysis of polyphosphate was also unaffected by light condition, but was reduced by the presence of  $\text{Ca}^{2+}$ . The released orthophosphates formed Ca-phosphate precipitates in the presence of  $\text{Ca}^{2+}$ , likely in amorphous phases. Results from this study lay the foundation for better understanding the chemical processes governing polyphosphate transport and transformation in various environmental settings.



### 1. INTRODUCTION

Polyphosphate is a type of phosphorus (P) species that is synthesized by all organisms, including a wide range of microorganisms (e.g., bacteria and plankton) in both terrestrial and marine settings.<sup>1–5</sup> Polyphosphates are polymers of at least three phosphate ions joined by phosphoanhydride ( $\text{P}=\text{O}-\text{P}$ ) bonds. They can occur in linear, ring (i.e., metaphosphates), or branched (i.e., ultraphosphates) structures. Polyphosphates can be extracellular or intracellular. During common cell events, such as extracellular release, lysis, death, and burial of microorganisms, polyphosphates are released into water bodies and can be incorporated into sediments. In fact, polyphosphates constitute a significant portion of total P in the dissolved phase, sinking particulates, and sediments, making them a key player in global P cycling.<sup>6–10</sup> In marine environment, polyphosphates were proposed to mediate the formation of calcium (Ca) phosphate minerals that are otherwise kinetically inhibited, thus playing a key role in the sequestration of biologically available P over geologic time scales.<sup>6,11</sup> Polyphosphates are also important industrial chemicals, frequently used in mineral processing (e.g., as a dispersant),<sup>12,13</sup> water treatment (e.g., for corrosion and scale prevention),<sup>14</sup> food industry (e.g., as preservatives, acidifying agents, acidity buffers, and emulsifying agents), and agricultural fertilizers.<sup>15</sup> These widespread industrial applications can ultimately result in the release of polyphosphates into soils and water bodies and potentially cause P contamination. Therefore, it is important to understand the transport and transformation of polyphosphates under various environmental settings.

Despite the industrial and biogeochemical significance of polyphosphates within the global P cycle, much remains unknown about the rate and mechanisms of its degradation and diagenesis. While previous studies have tracked polyphosphate concentrations in the field, details of the transformation process are not completely understood. For example, studies on lake sediments showed that polyphosphate rapidly disappeared at depth beyond 0.5 cm, indicating that polyphosphate was rapidly transformed or recycled.<sup>8</sup> Remineralization of polyphosphate was found to contribute a significant portion of soluble reactive phosphorus at the hypoxic/anoxic interface, suggesting the important role of polyphosphate in P cycling in this zone.<sup>7</sup> However, it is unclear how polyphosphates were transformed or recycled in these environments, as well as the relative importance of abiotic and biotic factors in controlling their stability and degradation. In comparison, extensive studies have been devoted to understanding the cycling of orthophosphate and organophosphorus. For example, it is well established that organisms release phosphate from organophosphorus compounds through enzymatic hydrolysis by various phosphatases.<sup>16–18</sup> Phosphatases are commonly synthesized and released by a wide range of bacteria and plankton, and their activities have been commonly detected in various environmental settings.<sup>16,17,19</sup> Given the ubiquitous existence of

Received: September 4, 2017

Revised: November 25, 2017

Accepted: January 3, 2018

phosphatases in soil and aquatic environments and the ability of some phosphatases to degrade polyphosphates,<sup>20</sup> it is important to understand the potential roles of phosphatases on the hydrolysis and transformation of polyphosphates. In this study, we characterized the rates and mechanisms of polyphosphate hydrolysis by several representative phosphatase enzymes as a function of polyphosphate chain length, the presence/absence of light, and the presence of  $\text{Ca}^{2+}$ .

## 2. EXPERIMENTAL SECTION

**2.1. Materials and Chemicals.** Polyphosphates (sodium salt) with average chain lengths of 15, 60, and 130 P units (hereafter referred to as 15P, 60P, and 130P) were generously provided by Dr. Toshikazu Shiba (Regenesis Inc., Tokyo, Japan). These polyphosphates were size fractionated and purified by gel electrophoresis and further characterized by gel permeation chromatography. Another polyphosphate with a broad chain length distribution (1–20 P units, average chain length of 6 units) was obtained from ICL Performance Products (MO, USA), which is labeled as soda polyphosphate. The average molecular weight of these polyphosphates was calculated based on an ideal molecular formula of  $\text{P}_n\text{O}_{(3n+1)}\text{Na}_{(n+2)}$  ( $n$  = number of P atoms in the molecule, that is, chain length). Polyphosphate stock solutions were prepared by dissolving an appropriate amount of polyphosphate in deionized (DI) water to achieve a concentration of 1 mg total mass per mL. Alkaline phosphatase from *Escherichia coli*, acid phosphatase from potato, and pyrophosphatase from yeast, were purchased from Sigma-Aldrich. Prior to the hydrolysis experiments, all enzyme stock solutions were prepared at the same concentration of 17 units/mL. On the basis of the information provided by the manufacturer, one unit of alkaline phosphatase can hydrolyze 1.0  $\mu\text{mol}$  of *p*-nitrophenyl phosphate per min at pH 10.4 at 37 °C; one unit of acid phosphatase can hydrolyze 1.0  $\mu\text{mol}$  of *p*-nitrophenyl phosphate per min at pH 4.8 at 37 °C; and one unit of pyrophosphatase can liberate 1.0  $\mu\text{mol}$  of inorganic orthophosphate per min at pH 7.2 at 25 °C. On the basis of optimal conditions for maximal enzymatic activities, alkaline phosphatase was dissolved in a Tris buffer solution (0.1 M, pH 8, with 5 mM  $\text{MgCl}_2$ ), while acid phosphatase and pyrophosphatase were dissolved in a HEPES buffer solution (0.01 M, pH 7, with 5 mM  $\text{MgCl}_2$ ).

**2.2. Enzymatic Hydrolysis.** To compare the effects of light condition and  $\text{Ca}^{2+}$  presence on phosphatase activities, four sets of enzymatic hydrolysis experiments were performed in parallel: (1) no light exposure (reaction containers wrapped by aluminum foil), (2) with light exposure (ambient lab lighting), (3) with light exposure and  $\text{Ca}^{2+}$  addition (1, 4, 10, and 20 mM  $\text{CaCl}_2$  in the final solution), and (4) with light exposure in buffered artificial seawater (ASW). ASW solution was prepared based on previous work<sup>21</sup> and contained 0.3 M  $\text{NaCl}$ , 50 mM  $\text{MgSO}_4$ , 10 mM  $\text{CaCl}_2$ , and 0.01 M  $\text{KCl}$ , at pH 7.0 (HEPES buffer), and 8.0 (Tris buffer) for acid and alkaline phosphatases, respectively. For all experiments, 9 mL of buffer solution (alkaline phosphatase 0.1 M Tris buffer, pH 8, with 5 mM  $\text{MgCl}_2$ ; acid phosphatase and pyrophosphatase 0.01 M HEPES buffer, pH 7, with 5 mM  $\text{MgCl}_2$ ) and 1 mL of 1 mg/mL polyphosphate stock solution were combined, and the reaction was initiated by adding 300  $\mu\text{L}$  of enzyme stock solution to reach a final enzyme concentration of ~0.5 unit/mL. Initial polyphosphate concentration was 100 mg of polyphosphate solids per L, equivalent to ~980  $\mu\text{M}$  orthophosphate for all

polyphosphates. The pH values of the reaction solutions were monitored throughout the experiments and found to be stable. At specific time points (0, 1, 2, 3, 4, 6, 8, 10, 24 h), 50  $\mu\text{L}$  solution was sampled and immediately analyzed for orthophosphate production using the phosphomolybdate colorimetric assay<sup>22</sup> on an UV-vis spectrometer (Carey 60, Agilent). All experiments were performed in an incubator at 37 °C in duplicate. Control experiments without enzyme addition were also performed in parallel, where only trace amount of orthophosphate was detected and remained constant throughout the experiments, likely from phosphate impurity in the original polyphosphate stock solutions. The effect of polyphosphate molar concentration on the hydrolysis rate of alkaline phosphatase was examined for a range of 60P and 130P concentrations.

Hydrolysis of polyphosphates in the presence of  $\text{Ca}^{2+}$  may induce Ca-phosphate precipitation. To monitor the initial nucleation and precipitation of Ca–P solid phases, 1 mL of the treatment suspensions in the absence or presence of alkaline phosphatase (from experiments #3 and #4) was transferred to a cuvette and monitored using dynamic light scattering (DLS, Malvern Zetasizer Nano ZS, Malvern Instruments, UK). White precipitates were collected via membrane filtration (0.4  $\mu\text{m}$ ) at the end of the experiment, rinsed with DI water, and air-dried for further structural characterization using scanning electron microscopy (SEM) and P K-edge X-ray absorption near edge structure (XANES) spectroscopy.

**2.3.  $^{31}\text{P}$  Nuclear Magnetic Resonance (NMR) Spectroscopy.** To characterize the transformation of polyphosphates during enzymatic hydrolysis, parallel experiments were conducted in liquid NMR sample tubes for  $^{31}\text{P}$  liquid NMR characterization. To obtain decent spectra within a reasonable time frame, higher concentrations of polyphosphates and enzymes were used. Briefly, 0.4 mL of buffers (0.1 M Tris buffer in the case of alkaline phosphatase, 0.01 M HEPES buffer for acid phosphatase and pyrophosphatase, with condition similar to the batch hydrolysis experiment) was combined with 0.2 mL of 1 mg/mL polyphosphate stock solution, 100  $\mu\text{L}$   $\text{D}_2\text{O}$ , and 40  $\mu\text{L}$  stock solution of enzymes in sample tubes. NMR spectra of these samples were collected at 0.5, 1, 2, 4, and 24 h reaction time at room temperature (22 °C). Liquid  $^{31}\text{P}$  NMR spectra were collected on a Bruker AMX 400 MHz spectrometer operated at 162 MHz and 297 K. A 90° pulse width, 6.5k data points (TD) over an acquisition time of 0.51 s, and relaxation delay of 15 s were applied. Chemical shift was calibrated using 85%  $\text{H}_3\text{PO}_4$  as the external standard. 64 scans were collected for each spectrum (equivalent to ~18 min).

**2.4. SEM.** For hydrolysis experiments conducted in the presence of  $\text{Ca}^{2+}$ , air-dried precipitates were spread onto carbon tape and characterized using an LEO 1530 SEM connected with energy dispersive spectrometer (Zeiss).

**2.5. P K-Edge XANES.** For hydrolysis experiments conducted in the presence of  $\text{Ca}^{2+}$ , air-dried precipitates were also analyzed by P K-edge XANES at beamline 14–3 at the Stanford Synchrotron Radiation Lightsource (SSRL), Menlo Park, CA. The powders were brushed evenly onto P-free Kapton tape and mounted to a sample holder maintained under helium atmosphere. XANES data were collected in fluorescence mode using a PIPS detector. Energy calibration used  $\text{AlPO}_4$  (edge position at 2152.8 eV). Two scans were collected for each sample and averaged for further analysis using the software Iffeffit.<sup>23</sup>

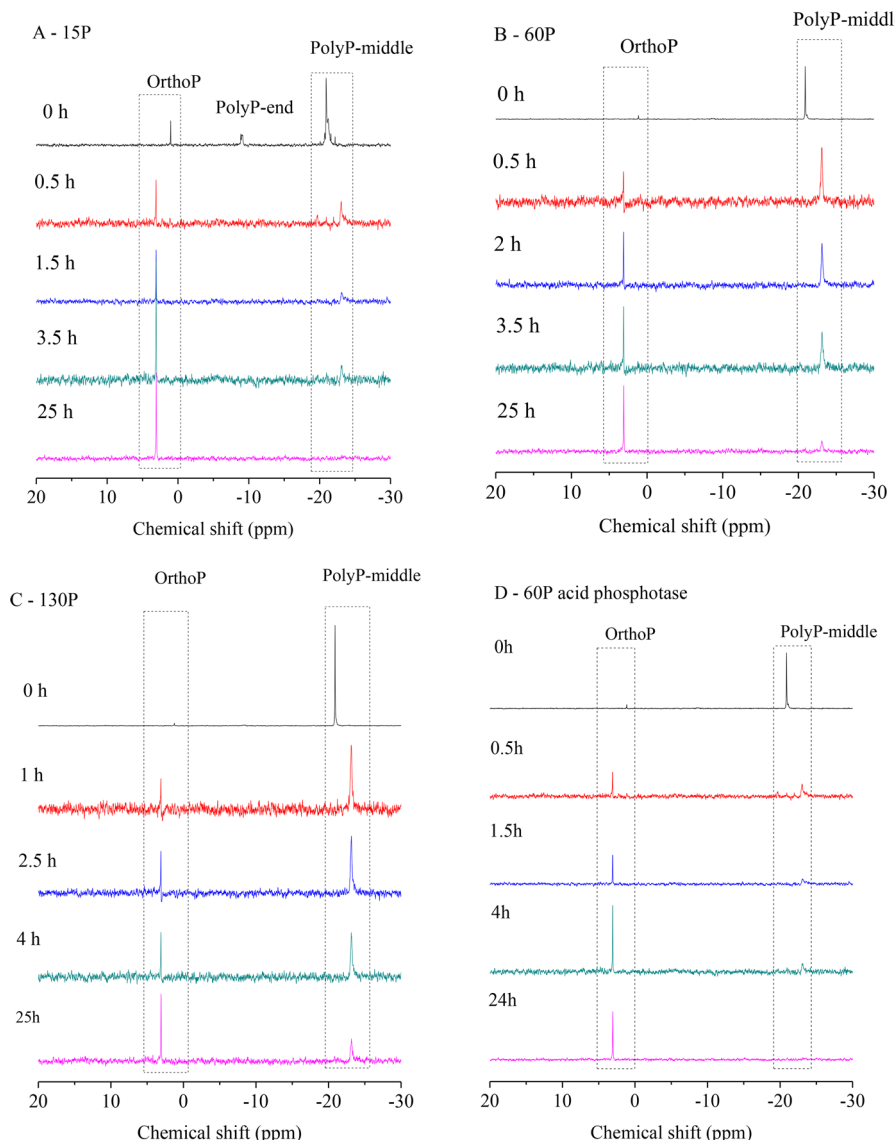


**Figure 1.** Time-resolved  $^{31}\text{P}$  liquid NMR spectra of 15P (A), 60P (B), and 130P (C) in the presence of alkaline phosphatase. The hydrolysis of 60P by acid phosphatase (D) was also monitored. Spectra (256 scans) at 0 h were recorded on stock solutions ( $\sim 0.86$  mg polyphosphate/mL) without buffer and enzyme addition. Only trace amounts of orthophosphate were present in all stock polyphosphate samples.

### 3. RESULTS AND DISCUSSION

**3.1. Hydrolysis Mechanism.**  $^{31}\text{P}$  NMR is a useful technique for differentiating P species with different molecular configurations. Because the middle ( $\text{P}_{\text{middle}}$ ) and end groups ( $\text{P}_{\text{end}}$ ) of polyphosphate molecules possess distinctive chemical shifts in the NMR spectrum (approximately  $-22$  and  $-7$  ppm, respectively),  $^{31}\text{P}$  NMR can be used to differentiate short and long chain polyphosphates by comparing the relative ratio of  $\text{P}_{\text{middle}}$  and  $\text{P}_{\text{end}}$  signals. We define  $\text{P}_{\text{end}}/\text{P}_{\text{total}}$  ratio as the relative abundance of end group P signal to the total signal from both end group and middle group P units. For longer chained polyphosphate molecules containing more middle group P units, this ratio is smaller than those of shorter chained polyphosphate molecules. As shown in Figure 1A, the spectrum of 15P polyphosphate showed a distinctive end group peak at about  $-7$  ppm, with a  $\text{P}_{\text{end}}/\text{P}_{\text{total}}$  ratio of  $\sim 0.15$  (close to  $2/15$ ). The end group signals for 60P and 130P polyphosphates were not evident, due to their small contribution to the total P signal (i.e.,  $\text{P}_{\text{end}}/\text{P}_{\text{total}}$  ratio of  $\sim 0.033$  and  $0.015$ , respectively) (Figure

1B and 1C). In comparison, a polyphosphate sample with a broad range of chain lengths showed slightly different chemical shifts of the  $\text{P}_{\text{middle}}$  groups, with multiple peaks at about  $-20$  ppm, as shown in Supporting Information (SI) Figure S1.

Given the linear structure of the studied polyphosphate molecules, it is possible that hydrolysis can occur via (1) random breakage of the phosphoanhydride ( $\text{P}-\text{O}-\text{P}$ ) bonds at terminal or middle groups or (2) one-by-one breakage of terminal  $\text{P}-\text{O}-\text{P}$  bonds only. These two pathways will lead to different P speciation profiles during enzymatic hydrolysis. If the phosphoanhydride bonds were randomly attacked by phosphatase (Mechanism 1), more polyphosphates (in terms of molecular concentration) with shorter chain lengths would form over time. As a result, the relative intensity of the end group signals in NMR spectra will increase accordingly, and the middle group signal may split. However, for all three polyphosphate samples with different chain lengths (15P, 60P, 130P),  $^{31}\text{P}$  liquid NMR spectra showed that over time there are (1) increase in the orthophosphate signal, (2) vanishing of the middle group signal, (3) little signal

contribution from the end groups, and (4) no multiple middle group peaks (Figure 1). Therefore, it is most likely that the enzyme molecules continuously hydrolyzed polyphosphate via its terminal groups, producing orthophosphate and shorter chained polyphosphates (mechanism 2). The enzymes can either continuously hydrolyze the same polyphosphate molecule until complete hydrolysis or switch to different polyphosphate molecules during this process. For 15P polyphosphate, although its end group signal was distinguishable at the beginning, the terminal-only pathway determines that a fraction of the 15P was completely degraded into orthophosphate, resulting in subsequent decrease of the 15P concentration (correspondingly end groups concentration) over time. This was observed by NMR as a gradual decrease of the  $P_{\text{end}}/P_{\text{total}}$  ratio over time (also see Figure S2). For longer chained polyphosphates, the  $P_{\text{end}}/P_{\text{total}}$  ratio was already small at the beginning, and this value further decreased as the polyphosphate concentration decreased. This is the reason that end group signals were not identified during the hydrolysis process for 60P and 130P. A similar phenomenon was observed during the hydrolysis of 60P by acid phosphatase, where only orthophosphate formed and no  $P_{\text{end}}$  peaks appeared following polyphosphate degradation (Figure 1D), suggesting a similar hydrolysis mechanism of acid phosphatase to alkaline phosphatase. Polyphosphate degradation was not observed in the presence of pyrophosphatase within 24 h (while pyrophosphate was completely degraded within 1 h under the same conditions), indicating that polyphosphate is not a target substrate for this enzyme (Figures S3 and S4).

Previous studies showed that the hydrolysis of organophosphorus by alkaline phosphatase involved the coupling of divalent cations (e.g.,  $Zn^{2+}$  and  $Mg^{2+}$ ) and the two charged oxygen of the phosphate groups to the active sites on the enzyme.<sup>24,25</sup> Given the structural configuration of linear polyphosphates, they are likely hydrolyzed in the same way as organophosphorus: only the terminal phosphate groups of the polyphosphates can be coupled to the active sites of the enzyme and subsequently hydrolyzed and released from the polyphosphate chain.

**3.2. Hydrolysis Kinetics: Effects of Chain Length and Substrate Concentration.** According to the terminal-only mechanism, one orthophosphate molecule is produced at each enzymatic hydrolysis step. This enables the quantification of the hydrolysis rate by measuring orthophosphate concentration over time. Results showed that the catalytic reactivity of acid phosphatase (tested at pH 7.0) toward 60P polyphosphate hydrolysis is higher than that of alkaline phosphatase (tested at pH 8.0), while pyrophosphatase has no reactivity toward the 60P polyphosphate (Figure 2). The hydrolyzing capacity of phosphatase enzymes varies with pH, and the classification of acid and alkaline phosphatases is based on the pH range in which their hydrolyzing activity reaches the maximum.<sup>17</sup> Although acid phosphatases are most reactive under acidic conditions (generally at pH 4–6), their activity at pH 7.0 remains high and is not lower than that of alkaline phosphatase, as shown in Figure 2. Even though alkaline phosphatases are generally considered to serve more extracellular functions,<sup>26</sup> acid phosphatases are also frequently found extracellularly,<sup>18,27</sup> and these results suggest that both groups of enzymes can play important roles in polyphosphate degradation under a range of environmentally relevant pH conditions.

In addition, polyphosphates with varied chain lengths (15P, 60P, 130P) were all rapidly hydrolyzed by alkaline phosphatase

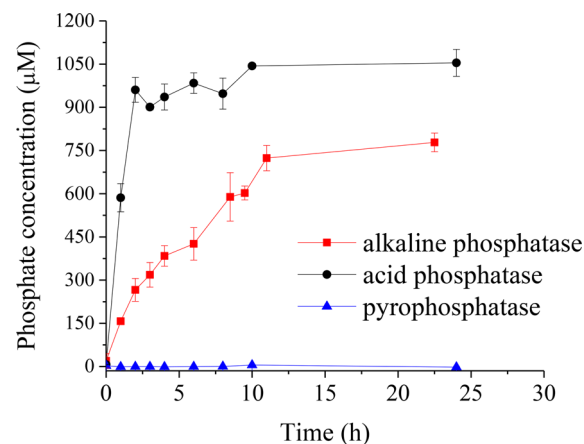


**Figure 2.** Enzymatic hydrolysis (quantified by orthophosphate production) of 60P polyphosphate by alkaline phosphatase, pyrophosphatase, and acid phosphatase. The starting concentrations for all polyphosphates were equivalent to 980  $\mu\text{M}$  phosphate, and the enzymes were at 0.5 unit  $\text{mL}^{-1}$ . Error bars represent the variation of duplicate experiments.

(Figure 3A). Both the rate and extent of orthophosphate production followed an order of 15P > 60P > 130P, due to a higher molecular concentration of the shorter chained polyphosphates at the same total P concentration (correspondingly more terminal phosphate groups available for reaction). This is consistent with the terminal-only mechanism. A random breakage pathway (mechanism 1) would have led to the overall increase of polyphosphate molar concentration over time (at least to a certain time point), which would have resulted in an exponential increase of the orthophosphate concentration due to increased probabilities of breakage at terminals to form orthophosphate. However, the rate data appeared as logarithmic-like curves that are characteristic of the depletion of substrates (Figure 3A), which supports the terminal-only pathway (mechanism 2).

With increasing concentration of polyphosphate substrates (60P and 130P), concentration of the produced orthophosphate increased, while the percentage of produced orthophosphate to total P decreased (Figure S5). This is possibly because (1) enzyme concentrations were set constant and became the rate-limiting factor at increasing substrate concentration and (2) enzyme activity was inhibited at increasing orthophosphate concentrations.<sup>16</sup> Figure 3B shows the phosphate production rate as a function of polyphosphate (60P and 130P) molar concentration in the presence of alkaline phosphatase. Orthophosphate formation rate was calculated by linear regression fitting of the initial points of Figure S5 (phosphate concentration within the first 4 h). In this case, since one substrate (i.e., polyphosphate molecules) is involved in multiple hydrolysis steps and led to the formation of multiple reaction products (orthophosphate and shorter-chained polyphosphates), we decided not to use the Michaelis–Menten equation to derive the Michaelis–Menten constants. However, as shown in Figure 3B, no difference was observed in the reactivity (i.e., phosphate production rate) of alkaline phosphate toward 60P and 130P degradation, suggesting that chain length does not affect the affinity of the polyphosphate molecules (or their terminal groups) to alkaline phosphatase enzyme molecules. Therefore, consistent with the terminal-only mechanism, the rate of enzymatic hydrolysis (or orthophosphate production rate) is dependent on the concentration of polyphosphate

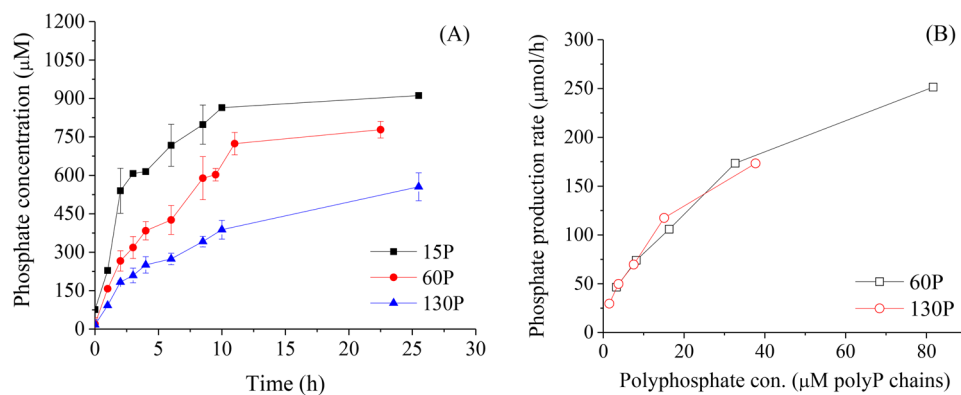


**Figure 3.** (A) Orthophosphate production as a function of time for polyphosphates with different chain lengths in the presence of alkaline phosphatase. (B) Orthophosphate production rate for 60P and 130P polyphosphates at varied molar concentrations in the presence of alkaline phosphatase. The starting concentrations for all polyphosphates were equivalent to 980  $\mu\text{M}$  phosphate, and the enzymes were at 0.5 unit  $\text{mL}^{-1}$ . Polyphosphate concentrations (molarity) in panel B were calculated by dividing the equivalent total phosphate concentration by average chain length. Kinetics of orthophosphate production for Figure 3B experiments is shown in Supporting Information (SI) Figure S5.

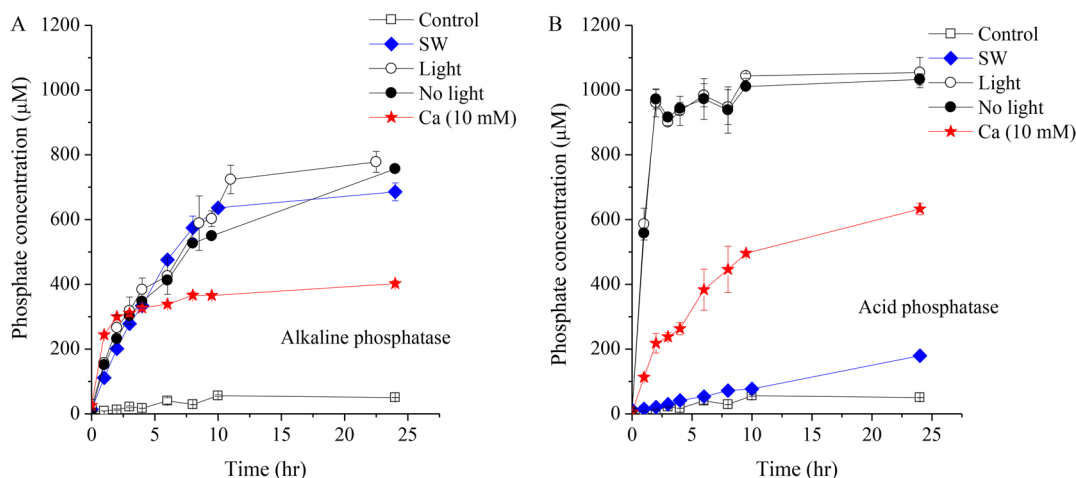


**Figure 4.** Hydrolysis of 60P polyphosphate mediated by (A) alkaline phosphatase and (B) acid phosphatase, under different light and solution conditions. The starting concentration of the 60P solutions was equivalent to 980  $\mu\text{M}$  phosphate. Control: 10 mM Ca buffer solution without enzyme. SW: Buffered artificial seawater. Ca (10 mM): 10 mM Ca buffer solution. Concentrations of enzyme = 0.5 unit  $\text{mL}^{-1}$ . Alkaline and acid phosphatases used Tris and HEPES buffers, respectively. Error bars represent the range of duplicate experiments.

terminal groups (correspondingly the molarity of linear polyphosphate chains), but not total P concentration.

**3.3. Hydrolysis Kinetics: Effects of Light and Solution Chemistry.** Previous studies have shown that the activity of alkaline phosphatase can be inhibited by enhanced UV-B radiation (280–320 nm) at 1.10  $\text{W m}^{-2}$ .<sup>28</sup> However, under the ambient lab lighting condition used in this study, light condition was observed to have little effect on the activity of both acid and alkaline phosphatases, as no substantial difference was observed in orthophosphate formation rates (Figure 4).

The presence of  $\text{Ca}^{2+}$  was found to substantially reduce the rates of orthophosphate production, with decreasing hydrolysis rate at elevated  $\text{Ca}^{2+}$  concentrations for both acid and alkaline phosphatases (Figures 4 and S6). This is unlikely due to Ca-phosphate precipitation, because no precipitation was observed at low  $\text{Ca}^{2+}$  ranges (1 and 4 mM) as observed by dynamic light scattering (Figures S6 and S7) and because precipitated phosphates are accounted for during the acidic orthophosphate measurement (precipitates dissolved). On the one hand,  $\text{Ca}^{2+}$  can precipitate with the hydrolysis product (orthophosphate) and remove it from the aqueous solution, which makes it kinetically favorable for polyphosphate hydrolysis. On the other

hand,  $\text{Ca}^{2+}$  and polyphosphate molecules can also form strong complexes (or even precipitates at relatively high concentrations),<sup>13,29</sup> which may inhibit the coupling of polyphosphate terminal groups to the active sites of the enzymes, subsequently inhibiting the enzymatic catalysis reaction. At the tested condition (980  $\mu\text{M}$  P,  $\text{Ca}^{2+}$  concentrations of 1, 4, 10, 20 mM), precipitation of Ca-polyphosphates did not occur at low  $\text{Ca}^{2+}$  concentrations (1 and 4 mM), but occurred at high  $\text{Ca}^{2+}$  concentrations (10 and 20 mM) according to dynamic light scattering observations (see section 3.4). It is possible that  $\text{Ca}^{2+}$  complexation with polyphosphates outpaced the effects of Ca-phosphate precipitation and lowered the overall hydrolysis rate. Another possible cause can be lowered enzymatic activity at increased  $\text{Ca}^{2+}$  concentrations.

Hydrolysis experiment in artificial seawater showed that the activity of alkaline phosphatase toward 60P hydrolysis remained high (comparable to the condition of  $\text{Ca}^{2+}$ -blank buffer, but higher than in 10 mM  $\text{Ca}^{2+}$  buffer), while the activity of acid phosphatase was substantially lower than in 10 mM  $\text{Ca}^{2+}$  buffer (Figure 4). This suggests that these two enzymes differ in their susceptibility to ionic strength, and that alkaline phosphatase-

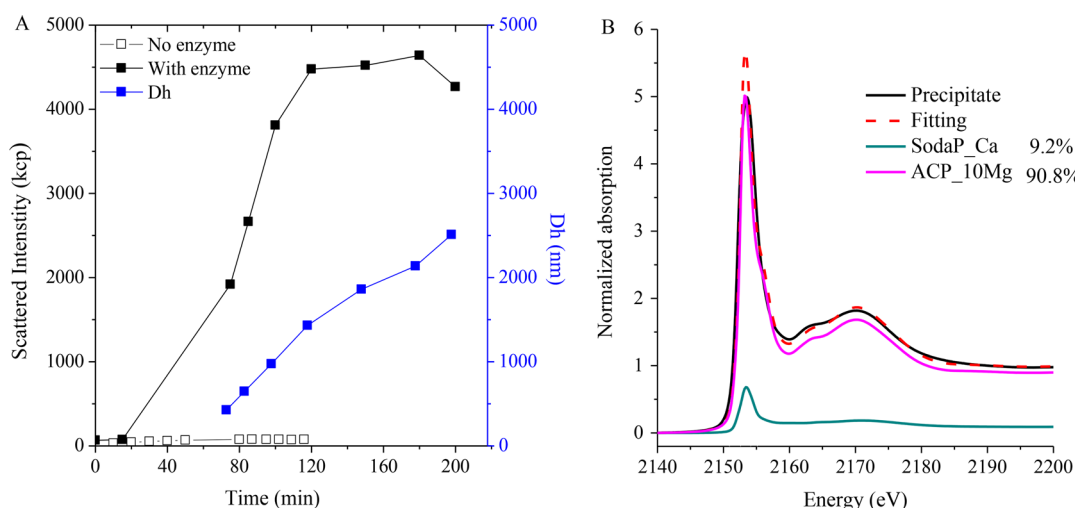


**Figure 5.** (A) Dynamic light scattering (DLS) measurements of the 15P hydrolysis experiments in the presence of 10 mM  $\text{Ca}^{2+}$ , with and without alkaline phosphatase addition. Dh is hydrodynamic diameter of the precipitates measured by DLS. (B) Linear combination fitting of P-XANES spectrum of the precipitates from the hydrolysis experiments in the presence of alkaline phosphatase and  $\text{Ca}^{2+}$ . Raw and fitted data are in black solid and red dotted lines, respectively. Best fit was obtained with 9.2% SodaP\_Ca (calcium salt of soda polyphosphate, a polyphosphate sample with a broad chain length distribution) and 90.8% ACP\_10Mg (Mg-doped amorphous calcium phosphate with  $\text{Mg}/(\text{Mg} + \text{Ca})$  ratio of 10%).

mediated polyphosphate hydrolysis is more relevant in marine environment.

In addition to  $\text{Ca}^{2+}$ , a variety of other factors have been found to affect the catalytic activity of phosphatase enzymes toward organophosphorus degradation, such as mineral adsorption and natural organic matter.<sup>30,31</sup> Further studies are needed to evaluate the effects of these environmentally relevant factors on polyphosphates hydrolysis.

**3.4. Hydrolysis Products in the Presence of  $\text{Ca}^{2+}$ .** In the presence of high  $\text{Ca}^{2+}$  concentration (10 and 20 mM), dynamic light scattering indicated the precipitation of solid phase, as evidenced by the increase of both particle size and light scattering intensity over time (Figures 5A and S7). In contrast, for control solutions in the absence of alkaline phosphatase, the light scattering intensity remained low and unchanged (Figure 5A), indicating the absence of precipitation due to the lack of polyphosphate degradation and orthophosphate formation. Therefore, precipitation is likely due to the formation of Ca-phosphate phases as a result of increasing orthophosphate concentration (from enzymatic hydrolysis of polyphosphates) and subsequent increase of oversaturation state with regard to Ca-phosphate solid phases. Indeed, P K-edge XANES spectrum of the precipitate showed distinctive features that are characteristic of Ca-phosphate phases (a secondary peak at  $\sim 2164$  eV and the oxygen oscillation centered at  $\sim 2170$  eV, although the post-edge shoulder is not as evident as that of crystalline Ca-phosphate phases) (Figures 5B and S8).<sup>32,33</sup> Linear combination fitting of the XANES data suggested that the precipitate has a structure similar to Mg-doped amorphous Ca phosphate phase (with 90.8% abundance) (Figure 5B). This is consistent with elemental analysis by energy dispersive X-ray spectroscopy (EDX), which suggested the precipitate to be a Ca–Mg–P phase with  $\text{Ca}:\text{Mg}$  molar ratio of  $\sim 10$  (Figure S9). The presence of  $\text{Mg}^{2+}$  in the precipitates is likely due to the presence of 5 mM  $\text{Mg}^{2+}$  in the reaction solution. Interestingly, no precipitation occurred for hydrolysis experiments conducted in artificial seawater, despite the presence of the same high  $\text{Ca}^{2+}$  concentration (10 mM) and a fast hydrolysis rate (Figures S6 and S7). This is likely due to high ionic strength (particularly

high  $\text{Mg}^{2+}$  concentration of 50 mM) in the artificial seawater that possibly inhibited  $\text{Ca}^{2+}$  phosphate precipitation.<sup>34–38</sup> Since  $\text{Mg}^{2+}$  is abundant in seawater (50 mM, as compared to 10 mM  $\text{Ca}^{2+}$ ) and has been found to inhibit the precipitation and crystallization of calcium phosphate minerals,<sup>34–38</sup> it is highly relevant to further explore the effects of  $\text{Mg}^{2+}$  on polyphosphate degradation and subsequent Ca-phosphate precipitation and transformation.

#### 4. IMPLICATIONS

Polyphosphate degradation is of great relevance to the cycling of polyphosphates of natural origin and from human activities. This study revealed the rates and mechanisms of polyphosphate hydrolysis by representative groups of phosphatase enzymes and as a function of polyphosphate chain length, light, and  $\text{Ca}^{2+}$ . In the absence of phosphatases, the tested polyphosphates are stable in aqueous solution under a broad range of pH conditions (without noticeable degradation even at pH 2.5 after one month, data not shown). Results from this work demonstrated that polyphosphates with a broad range of chain lengths can be rapidly degraded by both acid and alkaline phosphatases. Considering the ubiquitous presence of these enzymes in aquatic environments, enzymatic hydrolysis is likely to contribute to the rapid diagenesis of polyphosphates.<sup>8,39,40</sup>

The terminal-only enzymatic hydrolysis pathway suggests that polyphosphates can be potentially protected from enzymatic attack if the terminal phosphate groups are tightly complexed, for example, by cations or mineral surfaces. The released orthophosphate may be involved in processes, such as the precipitation of phosphate minerals (or precursors), surface adsorption, and utilization by organisms,<sup>10,41</sup> which will diversify the fate of the P derived from polyphosphate degradation.

Future studies are warranted to explore the influences of other environmental factors, such as additional aspects of solution chemistry and cation/mineral complexation, to better understand the transformation processes governing the fate of polyphosphates under varied environmental settings.

## ASSOCIATED CONTENT

### Supporting Information

The Supporting Information is available free of charge on the ACS Publications website at DOI: [10.1021/acs.est.7b04553](https://doi.org/10.1021/acs.est.7b04553).

$^{31}\text{P}$  liquid NMR spectra for various hydrolysis experiments and a polyphosphate sample with a broad range of chain lengths, various polyphosphate hydrolysis experiments including DLS data, P XANES spectra of different Ca–P phases, SEM image and energy dispersive X-ray spectrum (EDS) of the Ca–P precipitate, and two references ([PDF](#))

## AUTHOR INFORMATION

### Corresponding Author

\*E-mail: [yuanzhi.tang@eas.gatech.edu](mailto:yuanzhi.tang@eas.gatech.edu). Phone: 404-894-3814.

### ORCID

Yuanzhi Tang: [0000-0002-7741-8646](https://orcid.org/0000-0002-7741-8646)

### Author Contributions

<sup>#</sup>R.H. and B.W. contributed equally to this work.

### Notes

The authors declare no competing financial interest.

## ACKNOWLEDGMENTS

This work was supported by National Science Foundation under grants 1559087 and 1739884 (Y.T.) and 1559124 and 1736967 (J.M.D.). M.H. acknowledges support by National Nanotechnology Infrastructure Network Research Experience for Undergraduates (NNIN REU) program at Georgia Institute of Technology through NSF grant ECCS-0335765. We appreciate the help from Dr. Yongsheng Chen (Georgia Tech) for dynamic light scattering measurements and beamline scientist Matthew Latimer at SSRL Beamline 14-3 for help with P XANES experiment setup. Portions of this research were conducted at the Stanford Synchrotron Radiation Lightsource (SSRL). SSRL is a Directorate of SLAC National Accelerator Laboratory and an Office of Science User Facility operated for the U.S. Department of Energy Office of Science by Stanford University.

## REFERENCES

- Zhang, F.; Blasiak, L. C.; Karolin, J. O.; Powell, R. J.; Geddes, C. D.; Hill, R. T. Phosphorus sequestration in the form of polyphosphate by microbial symbionts in marine sponges. *Proc. Natl. Acad. Sci. U. S. A.* **2015**, *112* (14), 4381–4386.
- Martin, P.; Dyhrman, S. T.; Lomas, M. W.; Poulton, N. J.; Van Mooy, B. A. S. Accumulation and enhanced cycling of polyphosphate by Sargasso Sea plankton in response to low phosphorus. *Proc. Natl. Acad. Sci. U. S. A.* **2014**, *111* (22), 8089–8094.
- Kulakova, A. N.; Hobbs, D.; Smithen, M.; Pavlov, E.; Gilbert, J. A.; Quinn, J. P.; McGrath, J. W. Direct Quantification of Inorganic Polyphosphate in Microbial Cells Using 4'-6-Diamidino-2-Phenylindole (DAPI). *Environ. Sci. Technol.* **2011**, *45* (18), 7799–7803.
- Orchard, E. D.; Benitez-Nelson, C. R.; Pellechia, P. J.; Lomas, M. W.; Dyhrman, S. T. Polyphosphate in *Trichodesmium* from the low-phosphorus Sargasso Sea. *Limnol. Oceanogr.* **2010**, *55* (5), 2161–2169.
- Majed, N.; Matthäus, C.; Diem, M.; Gu, A. Z. Evaluation of Intracellular Polyphosphate Dynamics in Enhanced Biological Phosphorus Removal Process using Raman Microscopy. *Environ. Sci. Technol.* **2009**, *43* (14), 5436–5442.
- Diaz, J.; Ingall, E.; Benitez-Nelson, C.; Paterson, D.; de Jonge, M. D.; McNulty, I.; Brandes, J. A. Marine polyphosphate: A key player in geologic phosphorus sequestration. *Science* **2008**, *320* (5876), 652–655.
- Diaz, J. M.; Ingall, E. D.; Snow, S. D.; Benitez-Nelson, C. R.; Taillefer, M.; Brandes, J. A. Potential role of inorganic polyphosphate in the cycling of phosphorus within the hypoxic water column of Effingham Inlet, British Columbia. *Global Biogeochemical Cycles* **2012**, *26*, No. GB2040.
- Hupfer, M.; Ruübe, B.; Schmieder, P. Origin and diagenesis of polyphosphate in lake sediments: A  $^{31}\text{P}$ -NMR study. *Limnol. Oceanogr.* **2004**, *49* (1), 1–10.
- Martin, P.; Dyhrman, S. T.; Lomas, M. W.; Poulton, N. J.; Van Mooy, B. A. S. Accumulation and enhanced cycling of polyphosphate by Sargasso Sea plankton in response to low phosphorus. *Proc. Natl. Acad. Sci. U. S. A.* **2014**, *111* (22), 8089–8094.
- Diaz, J. M.; Björkman, K. M.; Haley, S. T.; Ingall, E. D.; Karl, D. M.; Longo, A. F.; Dyhrman, S. T. Polyphosphate dynamics at Station ALOHA, North Pacific subtropical gyre. *Limnol. Oceanogr.* **2016**, *61* (1), 227–239.
- Schulz, H. N.; Schulz, H. D. Large Sulfur Bacteria and the Formation of Phosphorite. *Science* **2005**, *307* (5708), 416–418.
- Papo, A.; Piani, L.; Ricceri, R. Sodium tripolyphosphate and polyphosphate as dispersing agents for kaolin suspensions: rheological characterization. *Colloids and Surfaces A: Colloids Surf., A* **2002**, *201* (1–3), 219–230.
- Rashchi, F.; Finch, J. A. Polyphosphates: A review their chemistry and application with particular reference to mineral processing. *Miner. Eng.* **2000**, *13* (10–11), 1019–1035.
- Lin, Y.-P.; Singer, P. C. Inhibition of calcite crystal growth by polyphosphates. *Water Res.* **2005**, *39* (19), 4835–4843.
- Kulakovskaya, T. V.; Vagabov, V. M.; Kulaev, I. S. Inorganic polyphosphate in industry, agriculture and medicine: Modern state and outlook. *Process Biochem.* **2012**, *47* (1), 1–10.
- Hoppe, H. G. Phosphatase activity in the sea. *Hydrobiologia* **2003**, *493* (1–3), 187–200.
- Jansson, M.; Olsson, H.; Pettersson, K. Phosphatases - Origin, Characteristics and Function in Lakes. *Hydrobiologia* **1988**, *170*, 157–175.
- Nannipieri, P.; Giagnoni, L.; Landi, L.; Renella, G., Role of Phosphatase Enzymes in Soil. In *Phosphorus in Action*, Bünemann, E., Oberson, A., Frossard, E., Eds.; Springer: Berlin, 2011; Vol. 26, pp 215–243.
- Ivancic, I.; Fuks, D.; Radic, T.; Lyons, D. M.; Silovic, T.; Kraus, R.; Precali, R. Phytoplankton and bacterial alkaline phosphatase activity in the northern Adriatic Sea. *Mar. Environ. Res.* **2010**, *69* (2), 85–94.
- Lorenz, B.; Schröder, H. C. Mammalian intestinal alkaline phosphatase acts as highly active exopolyphosphatase. *Biochim. Biophys. Acta, Protein Struct. Mol. Enzymol.* **2001**, *1547* (2), 254–261.
- Tang, Y. Z.; Webb, S. M.; Estes, E. R.; Hansel, C. M. Chromium(III) oxidation by biogenic manganese oxides with varying structural ripening. *Environ. Sci.-Process Impacts* **2014**, *16* (9), 2127–2136.
- Murphy, J.; Riley, J. P. A modified single solution method for the determination of phosphate in natural waters. *Anal. Chim. Acta* **1962**, *27*, 31–36.
- Ravel, á.; Newville, M. ATHENA, ARTEMIS, HEPHAESTUS: data analysis for X-ray absorption spectroscopy using IFEFFIT. *J. Synchrotron Radiat.* **2005**, *12* (4), 537–541.
- Holtz, K. M.; Kantrowitz, E. R. The mechanism of the alkaline phosphatase reaction: insights from NMR, crystallography and site-specific mutagenesis. *FEBS Lett.* **1999**, *462* (1–2), 7–11.
- Bamann, E.; Heumiiller, E. The activation of phosphatases by different metal ions. *Naturwissenschaften* **1940**, *28*, 535.
- Wilfert, P.; Kumar, P. S.; Korving, L.; Witkamp, G.-J.; van Loosdrecht, M. C. M. The Relevance of Phosphorus and Iron Chemistry to the Recovery of Phosphorus from Wastewater: A Review. *Environ. Sci. Technol.* **2015**, *49*, 9400–9414.
- Huang, X.; Morris, J. T. Distribution of phosphatase activity in marsh sediments along an estuarine salinity gradient. *Mar. Ecol.: Prog. Ser.* **2005**, *292*, 75–83.

(28) Garde, K.; Gustavson, K. The impact of UV-B radiation on alkaline phosphatase activity in phosphorus-depleted marine ecosystems. *J. Exp. Mar. Biol. Ecol.* **1999**, *238* (1), 93–105.

(29) Omelon, S.; Grynpas, M. Polyphosphates Affect Biological Apatite Nucleation. *Cells Tissues Organs* **2011**, *194* (2–4), 171–175.

(30) Zhu, Y.; Wu, F.; Feng, W.; Liu, S.; Giesy, J. P. Interaction of alkaline phosphatase with minerals and sediments: activities, kinetics and hydrolysis of organic phosphorus. *Colloids and Surfaces A: Colloids Surf., A* **2016**, *495*, 46–53.

(31) Mazzei, P.; Oschkinat, H.; Piccolo, A. Reduced activity of alkaline phosphatase due to host–guest interactions with humic superstructures. *Chemosphere* **2013**, *93* (9), 1972–1979.

(32) Oxmann, J. F. Technical Note: An X-ray absorption method for the identification of calcium phosphate species using peak-height ratios. *Biogeosciences* **2014**, *11* (8), 2169–2183.

(33) Ingall, E. D.; Brandes, J. A.; Diaz, J. M.; de Jonge, M. D.; Paterson, D.; McNulty, I.; Elliott, W. C.; Northrup, P. Phosphorus K-edge XANES spectroscopy of mineral standards. *J. Synchrotron Radiat.* **2011**, *18*, 189–197.

(34) Golubev, S. V.; Pokrovsky, O. S.; Savenko, V. S. Unseeded precipitation of calcium and magnesium phosphates from modified seawater solutions. *J. Cryst. Growth* **1999**, *205* (3), 354–360.

(35) Gunnars, A.; Blomqvist, S.; Martinsson, C. Inorganic formation of apatite in brackish seawater from the Baltic Sea: an experimental approach. *Mar. Chem.* **2004**, *91* (1), 15–26.

(36) Martens, C. S.; Harriss, R. C. INHIBITION OF APATITE PRECIPITATION IN MARINE ENVIRONMENT BY MAGNESIUM IONS. *Geochim. Cosmochim. Acta* **1970**, *34* (5), 621.

(37) Cao, X.; Harris, W. Carbonate and Magnesium Interactive Effect on Calcium Phosphate Precipitation. *Environ. Sci. Technol.* **2008**, *42* (2), 436–442.

(38) Ferguson, J. F.; McCarty, P. L. Effects of carbonate and magnesium on calcium phosphate precipitation. *Environ. Sci. Technol.* **1971**, *5* (6), 534–540.

(39) Sannigrahi, P.; Ingall, E. Polyphosphates as a source of enhanced P fluxes in marine sediments overlain by anoxic waters: Evidence from P-31 NMR. *Geochem. Trans.* **2005**, *6* (3), 52–59.

(40) Martin, P.; Lauro, F. M.; Sarkar, A.; Goodkin, N.; Prakash, S.; Vinayachandran, P. N. Particulate polyphosphate and alkaline phosphatase activity across a latitudinal transect in the tropical Indian Ocean. *Limnol. Oceanogr.* **2018**, DOI: 10.1002/lno.10780, in press.

(41) Moore, L.; Ostrowski, M.; Scanlan, D. J.; Feren, K.; Sweetsir, T. Ecotypic variation in phosphorus-acquisition mechanisms within marine picocyanobacteria. *Aquat. Microb. Ecol.* **2005**, *39*, 257–269.